

Cryo-Infrared Optical Characterization at NASA GSFC

Ray Boucarut¹, Manuel A. Quijada², and Ross M. Henry¹
¹Goddard Space Flight Center, Code 551, Greenbelt, MD 20771
 ray.boucarut@gsfc.nasa.gov
²Swales Aerospace, Beltsville, MD 20705

ABSTRACT

The development of large space infrared optical systems, such as the Next Generation Space Telescope (NGST), has increased requirements for measurement accuracy in the optical properties of materials. Many materials used as optical components in infrared optical systems, have strong temperature dependence in their optical properties. Unfortunately, data on the temperature dependence of most of these materials is sparse. In this paper, we provide a description of the capabilities existing in the Optics Branch at the Goddard Space Flight Center that enable the characterization of the refractive index and absorption coefficient changes and other optical properties in infrared materials at cryogenic temperatures. Details of the experimental apparatus, which include continuous flow liquid helium optical cryostat, and a Fourier Transform Infrared (FTIR) spectrometer are discussed.

1.0 Introduction

Optical Component testing and verification are essential aspects of optical technology development for far-infrared and sub-millimeter astronomy. The NASA Goddard Far-Infrared laboratory has historically supported optical instrument development in the atmospheric science and infrared astronomy program areas. Since the early 1980's a variety of NASA and Space science programs have been supported including the COBE (Cosmic Background Explorer), the Space Infrared Telescope Facility (SIRTF) Infrared Array Camera (IRAC) the Composite InfraRed Spectrometer (CIRS) and technology development for the Next Generation Space Telescope (NGST) (Table 1). These programs were supported through far-infrared and sub-millimeter measurements at temperature ranging from room to 1.4 K

Figure 1 shows the importance and necessity of these measurements. A temperature shift in the spectral transmittance curve of filter 1 for the SIRTF/IRAC filter is seen between 3 and 4 microns. This shift was seen in many of the filters for this instrument. Figure 2 shows the results of the spectral calibration of Goddard's KAO spectrometer used to measure the first Far - IR spectrum of Supernova SN 1987A.

2.0 Capabilities

The heart of the Far-Infrared measurement facility is the Fourier Transform Infrared Interferometer. A Bruker IFS 113V(Genzel interferometer – Figure 5) and Nicolet 8000 (Michelson interferometer) have been used. The current instrument is the Bruker (Figure 4). The Bruker has a spectral range from 250 nm up to 2.5 mm or 4 cm^{-1} to 40000 cm^{-1} . A grating

spectrometer spanning the 200 nm to 3 μm region complements the available instruments. (Perkin-Elmer Lambda 9). All of these instruments are capable of transmission and reflection measurements at variable angles of incidence. A variety of cryostats are available for cooling the samples from room to liquid helium temperatures.

3.0 Materials Studies

The Far-Infrared laboratory has been involved extensively in studying optical properties of materials at far infrared wavelengths. These studies include the measurement of the optical properties of crystal substrates and of metal mesh filters. The filter development program for the Diffuse Infrared Background Experiment (DIRBE) on the Cosmic Background Explorer Satellite (COBE) afforded the opportunity to measure the transmission of numerous materials warm and cold. Many of these materials became part of the filter stack on DIRBE.¹⁻³ Other materials were used as blocking filters during measurements. The results of these measurements are shown in figure 6 and 7.

Numerous studies were made on the reflectivity of various black paints. Black paints are used for suppression of stray light in optical instrument. The behavior of black paint in the far infrared is not well known. Figure 8 plots on a log-log scale the relative specular reflectance of numerous black paints measured. The spectral range of the measurements is from 1 to 1000 microns.

Additional tests have been made on high temperature superconductors. Figure 9 shows the reflectance of $\text{Nd}_{1.85}\text{Ce}_{0.15}\text{CuO}_{4-g}$ between 100 and 1000 microns. The data was taken at 8 and 25 K. The rising reflectance is an indication of the sample undergoing a transition from the normal to the superconducting state⁵. Spectra has also been taken of cyanoacetylene and cyanogens samples for comparison with measurements of the spectra of Titan's atmosphere (Figure 10). Metal mesh filters hold much promise as filters for far-infrared spectroscopy⁶. In figure 11 are plots of two different types of mesh filters: inductive and capacitive. Both types of constructions were measured for transmittance both at room and cryogenic temperatures. Figure 12 shows a comparison between theoretical models for and laboratory measurements for conductive and inductive meshes with different geometric factors.

NASA PROGRAMS INVOLVING FAR-IR AND CRYO- OPTICS

Project	Fore Optics Temperature	Focal Plane	Wavelength
COBE	3 K	2 K	10 μm – 3 cm
IRAS	3 K – 10 K	< 3 K	8 μm – 300 μm
CLIR	30 K	10 K	2.5 μm – 25 μm
SIRTF/IRAC	1.4 K	17 K	3 μm – 10 μm
CIRS	170 K	80 K	7 μm – 1000 μm
NGST	30 K	< 8 K	0.5 – 20 μm

Table 1 . Goddard's Far infrared measurement laboratory has supported optical instrument development in a variety of infrared astronomy program areas

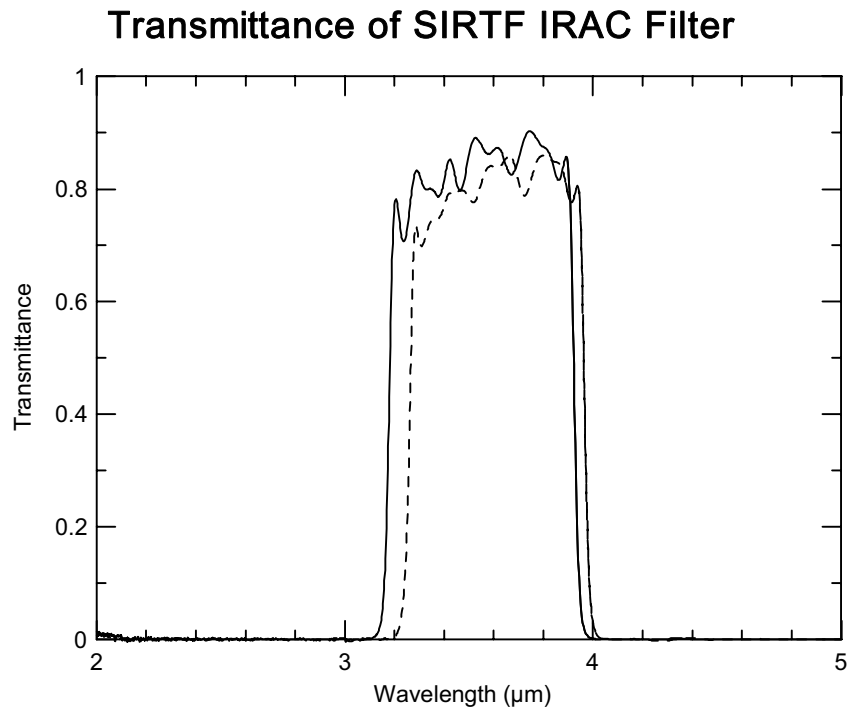


Figure 1. The transmittance of SIRTF/ IRAC Filter 1 measured at room temperature (dashed) and at 5 K (solid) and at an angle of incidence of 11 $^{\circ}$.

Spectral Bands in the GSFC KAO Spectrometer
 Used to Measure the First Far-IR Spectrum of
 Supernova SN1987A

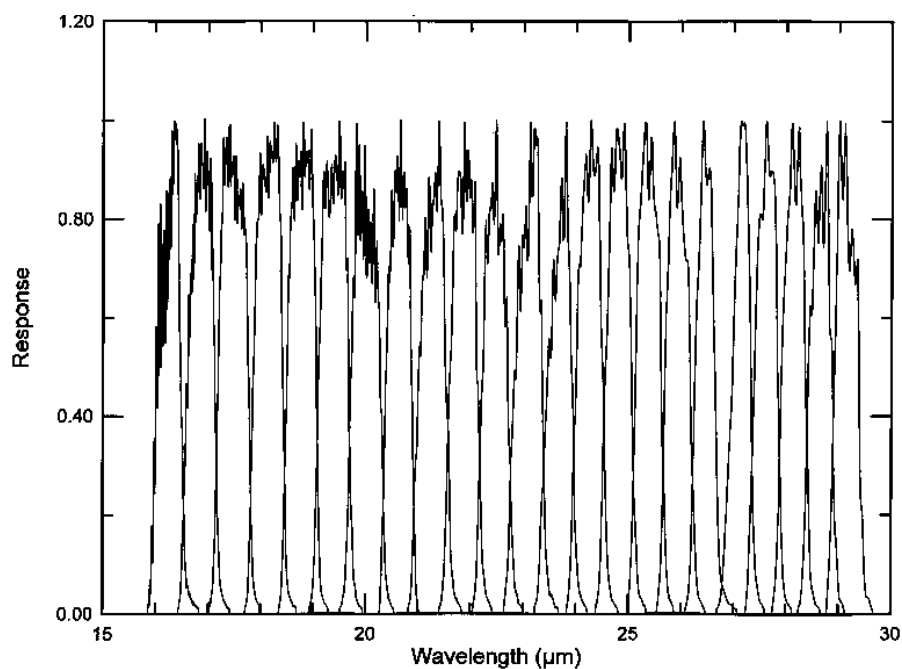


Figure 2. Spectral bands measured in the KAO Spectrometer

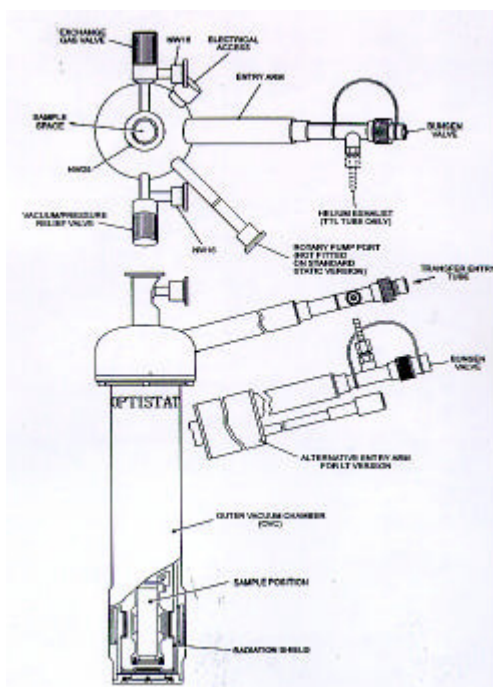


Figure 3. Diagram of Oxford Cryostat

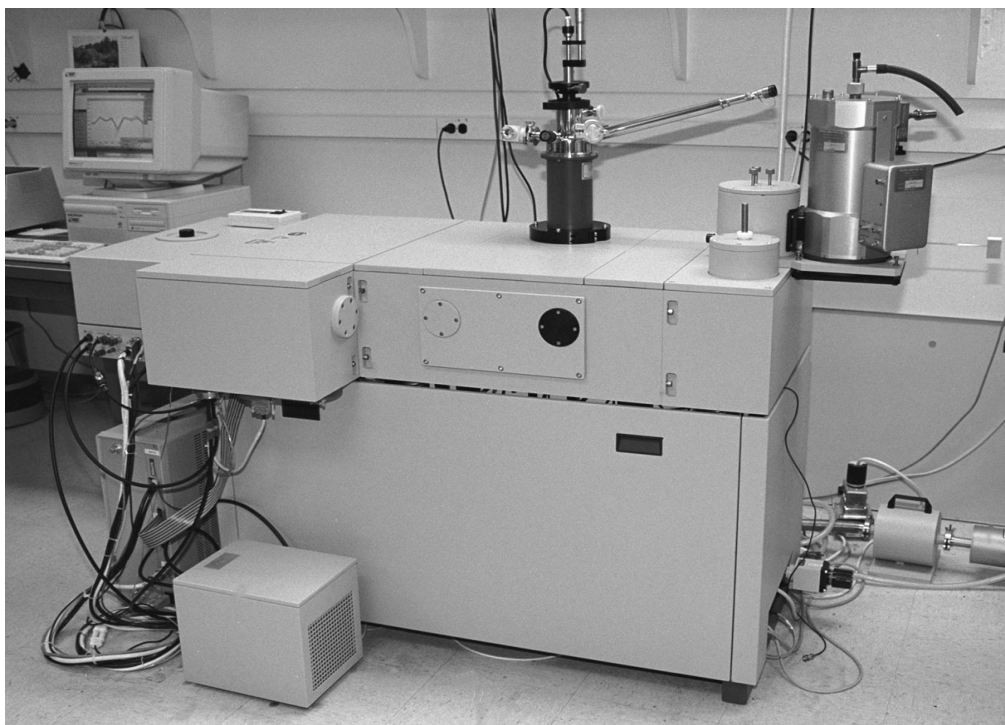


Figure 4. Bruker FTIR Spectrometer, wavelength range from 250 nm to 2 mm, Maximum resolution - 0.03 cm^{-1}

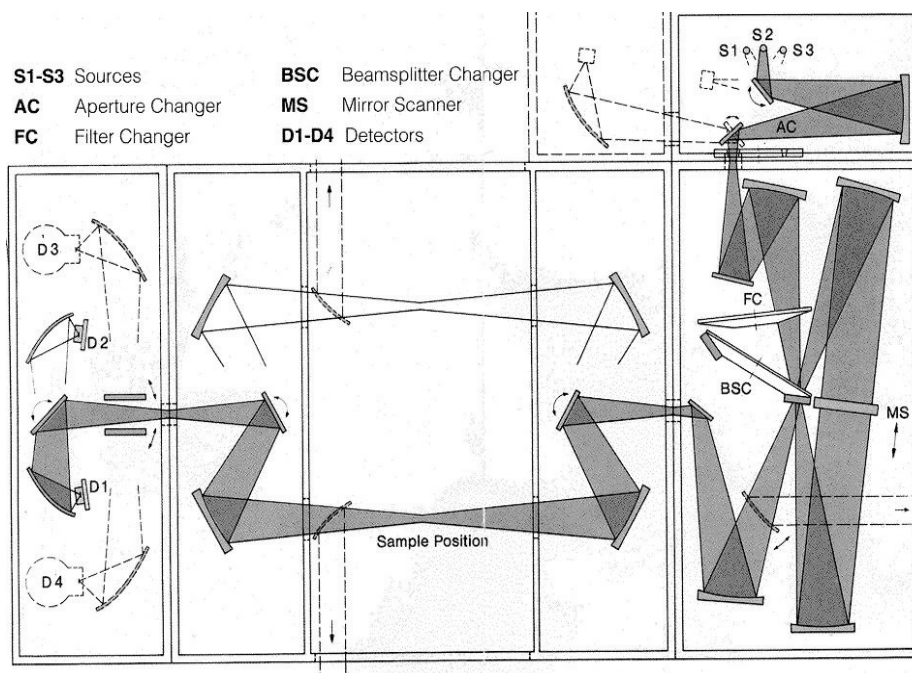


Figure 5. Layout of Genzel spectrometer

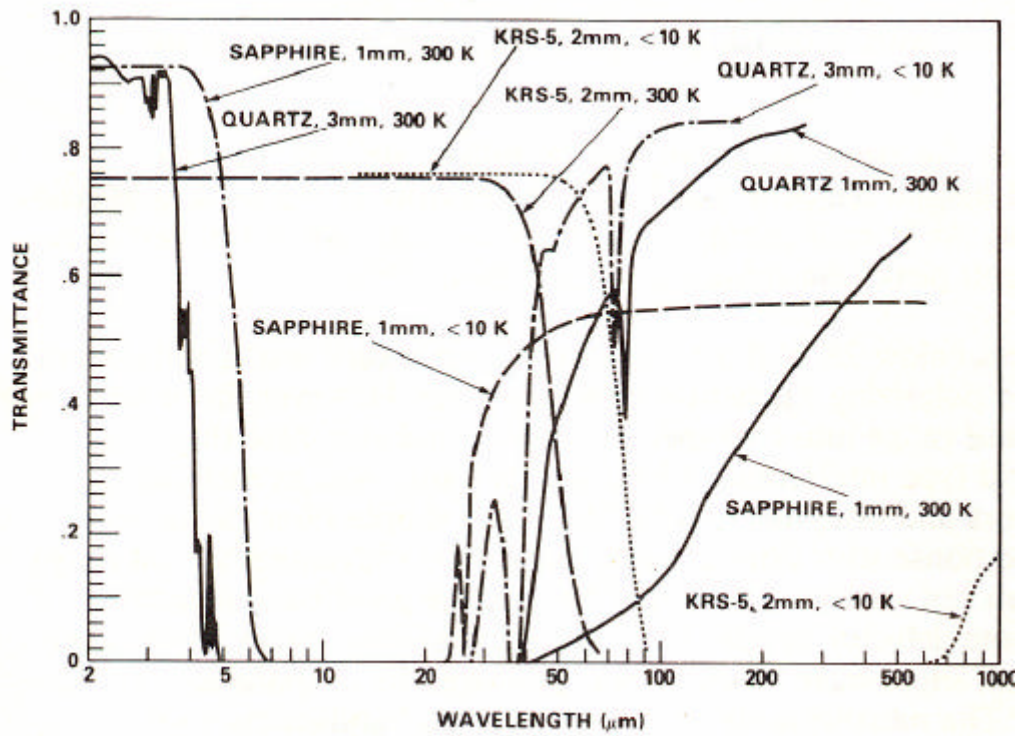


Figure 6. Transmittances of KRS-5, sapphire and crystalline quartz over the 1mm to 1000mm wavelength region at temperatures of 300K and below 10K.

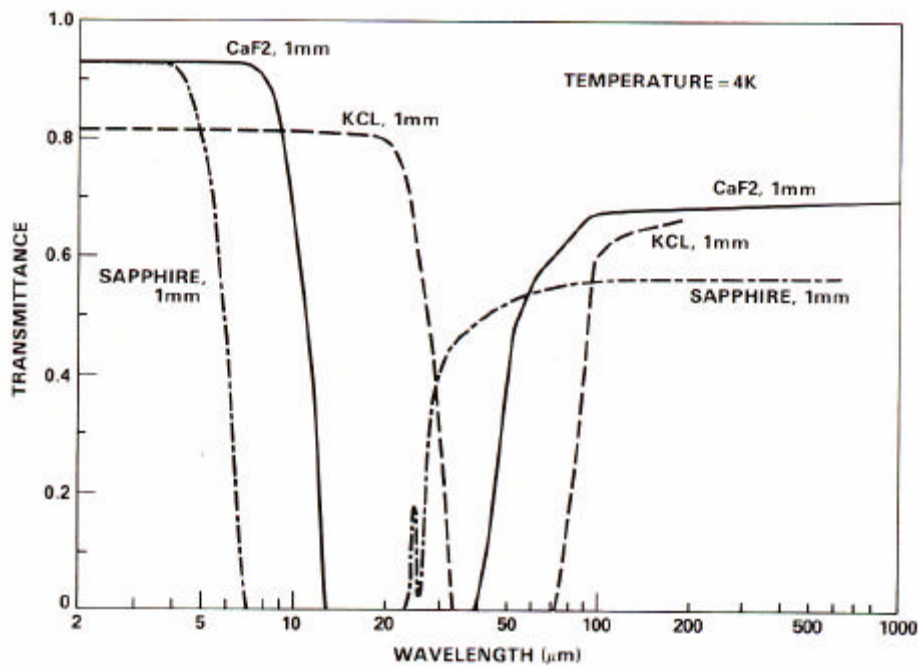


Figure 7. Transmittance of 1 mm thick sapphire, CaF. and KCl over the 2mm to 1000mm wavelength region at a temperature of 4K

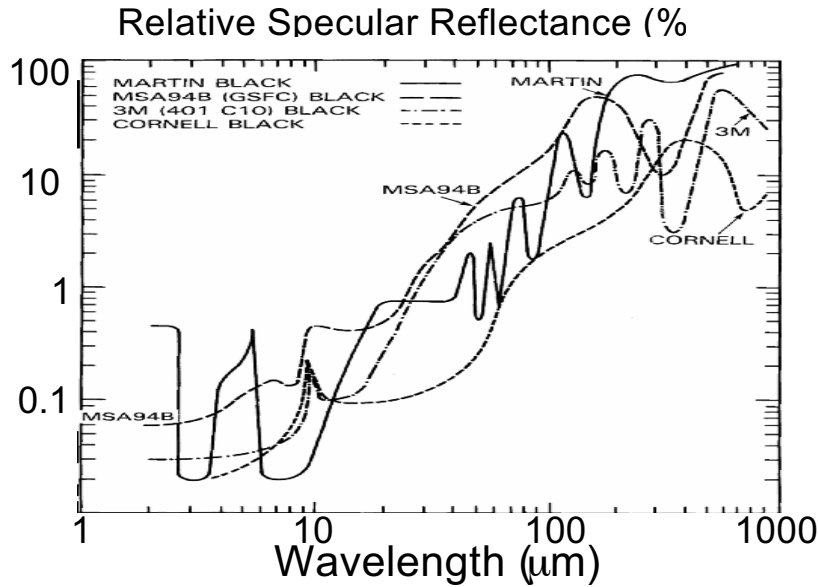


Figure 8. Relative specular reflectance of various black paints measured in Goddard's Far IR measurement laboratory. Wavelength range 1 to 1000 microns. Reflectance displayed on a logarithmic scale.

High Temperature Superconductor, $\text{Nd}_{1.85}\text{Ce}_{0.15}\text{CuO}_{4-g}$ $T_c = 21 \text{ K}$

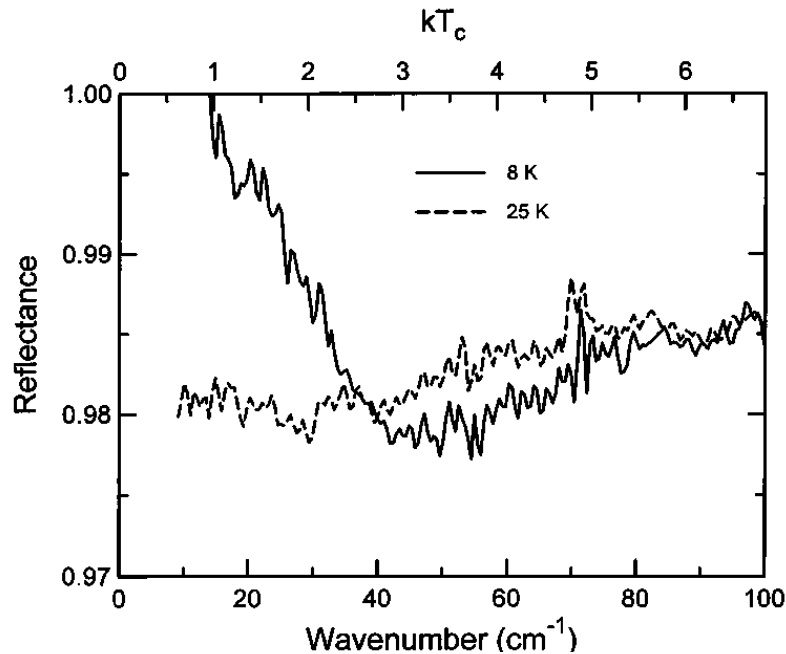


Figure 9. This figure shows changes in the reflectance as function of frequency for a high-temperature superconductor material above (25 K) and below (8 K) the critical transition temperature ($T_c \sim 12 \text{ K}$). Notice the rising reflectivity of the sample at low frequencies and for measurements done at $T = 8 \text{ K}$. This is an indication that the sample is in the superconducting state.

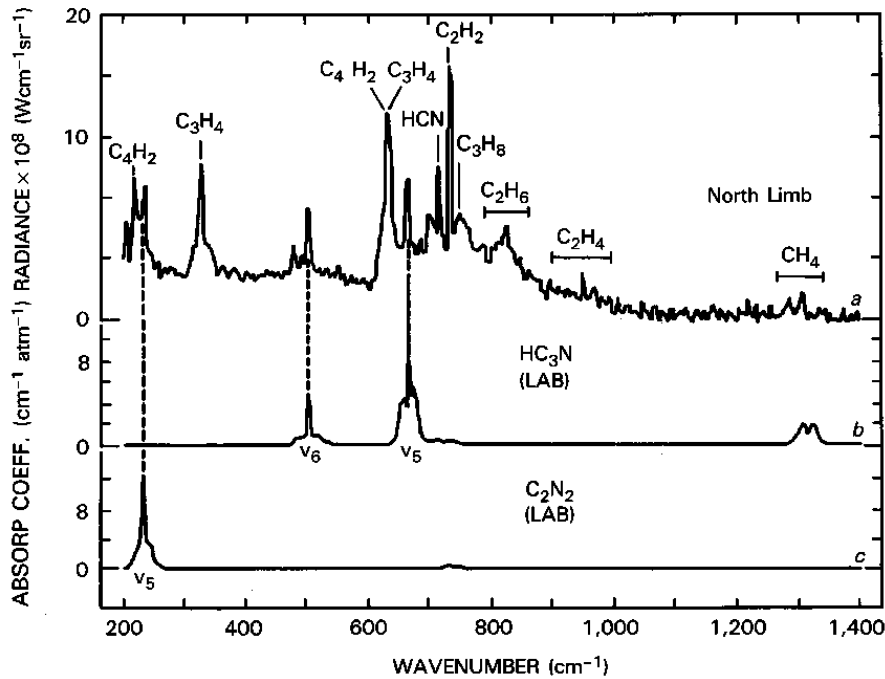


Figure 10. Voyager Titan Spectrum - Comparison of laboratory and Titan radiance spectra. The observed spectrum (a) was obtained off the limb of the planet in the northern polar cap region. The high air mass along the line of sight enhances the weak emission features, while space contamination in the field of view depresses the adjacent continuum. Laboratory spectra for cyanoacetylene (HC_3N) (b) and cynogen (C_2N_2) (c) are shown.

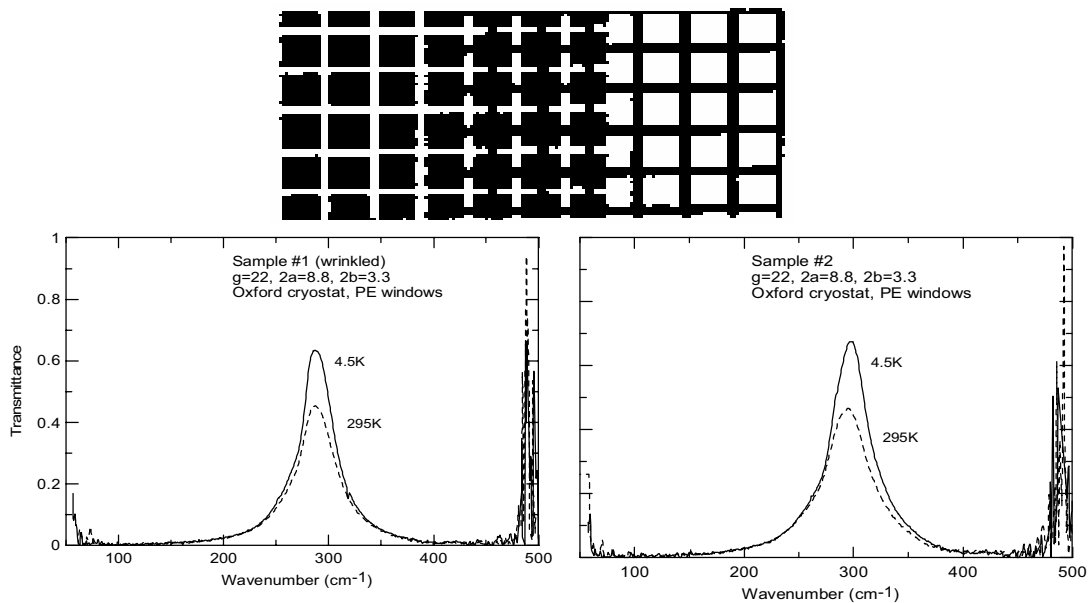


Figure 11. Production of cross shaped pattern (middle region) by superposition of a capacitive (left) and an inductive (right) grids. The dark regions represent metallic conducting areas, whereas the clear regions are dielectric insulating material.

Temperature dependence in the spectral transmittance for two inductive grids (labeled Sample #1 and #2 respectively) on a 2 μm thick polyimide substrate. The geometrical factors or grid parameters g , $2a$ and $2b$ can be defined in terms of the cross pattern shown in the middle section of previous figure: g is periodicity of the crosses, $2a$ is separation between crosses, and $2b$ is size or width of crosses

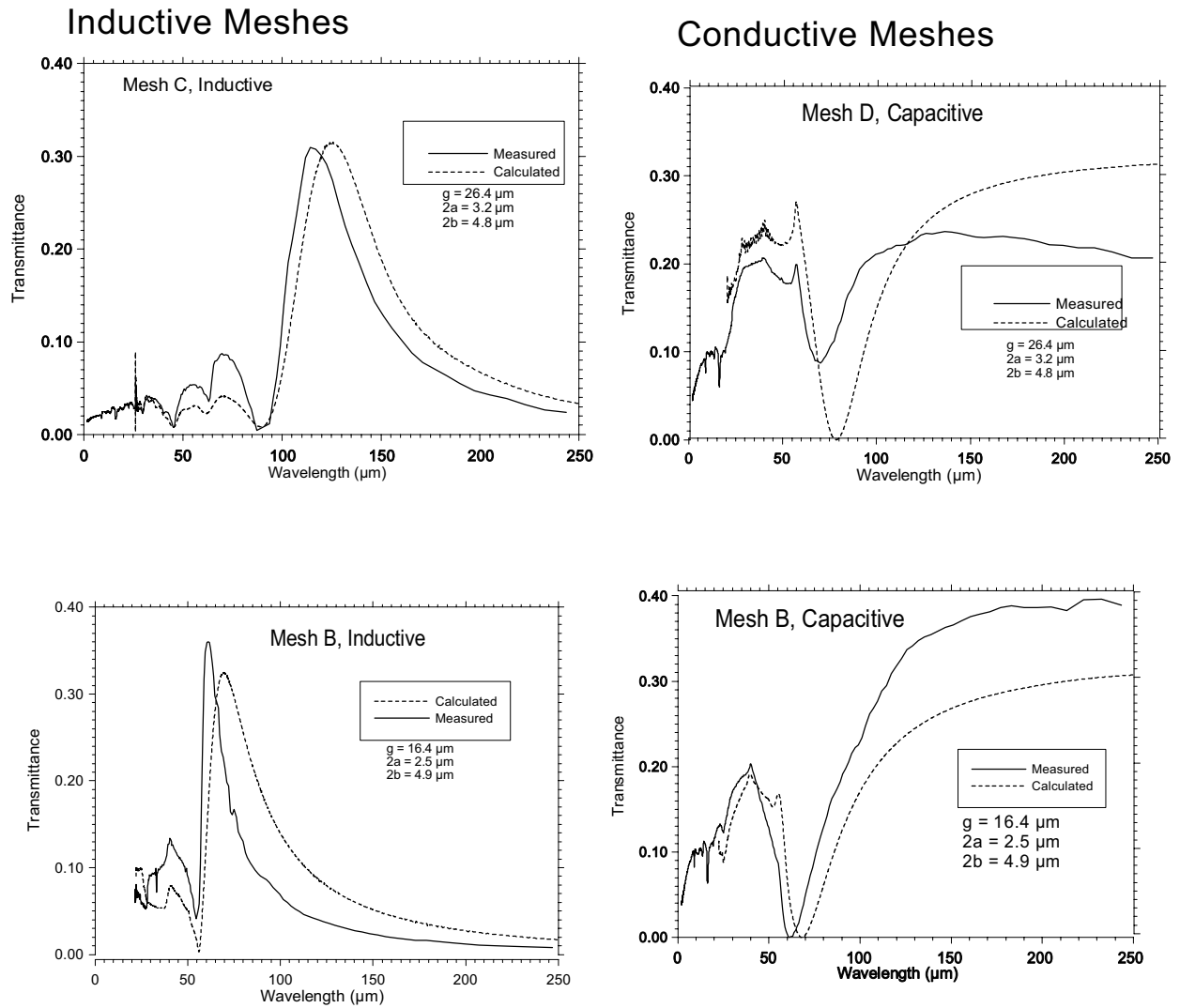


Figure 12. Inductive Meshes (Left side figures)

Comparison between the measured and calculated transmittance as a function of wavelength for two different inductive meshes, labeled C & B respectively, along with their geometrical factors g , $2a$, and $2b$.

Capacitive Meshes (Right side figures)

Comparison between the measured and calculated transmittance as a function of wavelength for two different capacitive meshes, labeled D & B respectively, along with their geometrical factors g , $2a$, and $2b$.

4.0 References

1. K. P. Stewart, M. A. Quijada, "Cryo -transmittance and reflectance of filters and beamsplitters for the SIRTf Infrared Array Camera," SPIE proceedings, 4131, 218 -227, (2000)
2. J. B. Heaney, K. P. Stewart, R. A. Boucarut, "The Cryo-Testing of Infrared Filters and Beamsplitters for the Cosmic Background Explorer's Instruments", SPIE VOL. 619, 142 - 147 (1986)
3. J. B. Heaney, R. A. Boucarut, K. P. Stewart, "Infrared filters for cryogenic Radiometers", Cryogenic Optical Systems and Instruments V, 118-130, 1993
4. K. D. Moller, R. G. Zoeller, N. G. Ugras, P. Zablocky, J. B. Heaney, K. P. Stewart and R. A. Boucarut, "Noise tube sources for the far IR and millimeter region", Applied Optics, Vol. 27, No. 10, 1988
5. K. P. Stewart, Ph. D. dissertation, University of Maryland (1997)
6. K. D. Moller, J. B. Warren, J. B. Heaney, C. Kotecki, "Cross -shaped bandpass filters for the near- and mid-infrared wavelengths regions", Applied Optics 35(31), 6210 -6215 1996